Journal of ELECTRONIC MATERIALS, Vol. 47, No. 8, 2018
https://doi.org/10.1007/s11664-018-6362-y
© 2018 The Minerals, Metals & Materials Society

Effect of Shock Waves on Dielectric Properties of KDP Crystal

A. SIVAKUMAR,[1] S. SURESH,[1] J. ANTO PRADEEP,[1] S. BALACHANDAR,[2] and S.A. MARTIN BRITTO DHAS[1,3]

1.—Department of Physics, Abraham Panampara Research Center, Sacred Heart College, Tirupattur, Tamilnadu 635601, India. 2.—Department of Research and Development, AKSH Optifibre Private Limited, Bhiwadi, Rajasthan 301019, India. 3.—e-mail: brittodhas@gmail.com

An alternative non-destructive approach is proposed and demonstrated for modifying electrical properties of crystal using shock-waves. The method alters dielectric properties of a potassium dihydrogen phosphate (KDP) crystal by loading shock-waves generated by a table-top shock tube. The experiment involves launching the shock-waves perpendicular to the (100) plane of the crystal using a pressure driven table-top shock tube with Mach number 1.9. Electrical properties of dielectric constant, dielectric loss, permittivity, impedance, AC conductivity, DC conductivity and capacitance as a function of spectrum of frequency from 1 Hz to 1 MHz are reported for both pre- and post-shock wave loaded conditions of the KDP crystal. The experimental results reveal that dielectric constant of KDP crystal is sensitive to the shock waves such that the value decreases for the shock-loaded KDP sample from 158 to 147. The advantage of the proposed approach is that it is an alternative to the conventional doping process for tailoring dielectric properties of this type of crystal.

Key words: Shock tube, shock wave loading, KDP crystal, dielectric properties

INTRODUCTION

In realistic modeling for microelectronic and optoelectronic industrial applications, it is essential that we understand the performance of crystals in bulk or nano form in extreme conditions. Knowledge of solid-state physics and atomic structure regarding parameters such as stability, pressure, temperature, vibration, thermal shock, and mechanical shock are critical.[1–3] The effects of dielectric properties under static high pressure and high temperature conditions are well known, especially dielectric properties of lamellar thiophosphate ($CuInP_2S_6$), lead titanate ($PbTiO_3$) crystals; which exhibit the ferroelectric phase transition under high pressure.[4,5] Kedyulich et al. investigated temperature and pressure effects on the anisotropy of dielectric permeability in KDP and deuterated potassium dihydrogen phosphate (DKDP) crystals.[6,7] A shock wave is a type of dynamic impulse with high temperature and high pressure, and the shock compression process applies a dynamic stress on materials with a simultaneous heating effect. It is well known that under the impact of shock waves or a shock layer, the high pressure and high temperature can result in a variety of chemical and physical transformations in solids. Internationally, many research groups are working in the field of shock waves, in both theoretical and experimental research, since they have tremendous potential applications. The literature reports that in single crystals, plane shock wave exposure induces elastic compression, plastic deformation, structural and phase transformation, change in transparency, refractive index, resistivity, etc.[8–17] Kadu et al. demonstrated shock wave-induced phase transformation and change in the grain orientation of iron and its alloys.[18,19] The property of mechanoluminescence and electrical resistivity of the quartz crystal decreases under increasing shock wave pressure.[20] Shock wave

(Received September 8, 2017; accepted May 5, 2018; published online May 22, 2018)

interaction in crystals creates micro or macro level structural changes which can alter mechanical, optical, electrical and thermal properties of a material. Among these, the tuning of dielectric properties of materials is expected to play an important role in developing new materials for technological applications. Since materials of low dielectric constant are very suitable for microelectronic and optoelectronics applications, tuning the dielectric behavior of a potential material to a lower level without affecting its other properties is a challenging and interesting field.[21] KDP crystal is one of the remarkable ferroelectric materials, as it possesses well known non-linear optical properties as well as outstanding physical properties. It is used in telecommunication, optoelectronic, microelectronic and high power laser technology.[22–24] There is no literature available describing the effect of shock wave loading conditions for KDP crystal. In this article, the effect of shock waves on dielectric properties of KDP crystal is discussed.

EXPERIMENTAL SECTION

A single crystal of KDP with dimension $27 \times 12 \times 3.6$ mm^3 was grown by the slow evaporation method from a saturated solution in a period of 4 weeks. A test-sample of KDP (100)[25,26] was cut and polished in the plane of window size $13.1 \times 11.5 \times 3.3$ mm^3 (Fig. 1) and subjected to a couple of shock waves. The shock waves were produced by a table-top pressure driven shock tube which was fabricated in our laboratory. It is an efficient device for producing controlled shock waves in laboratory conditions. It consists of three sections: the driver section (higher-pressure section), the driven section (lower-pressure section) and a diaphragm section which couples the other two sections. Using a bicycle pump, ambient air was periodically compressed and subsequently fed into the driver section until the diaphragm ruptured. This created a shock wave which propagated through the driven section. The test sample was rigidly fixed in the sample holder which was placed 2 cm away from the open end of the driven section. A schematic diagram of the experimental setup is shown in Fig. 2. By this means, couple of shock waves were loaded on the KDP sample with the pulse width around 1.47 s, having transient pressure of 1280 kPa (128 N/cm^2), transient temperature of 699 K and Mach number 1.9. The transient pressure profile of shock wave Mach number 1.9 is shown in Fig. 3. The pressure and temperature of the shock waves were evaluated by standard R–H shock wave relations[27]; the shock tube was calibrated before conducting the experiment.

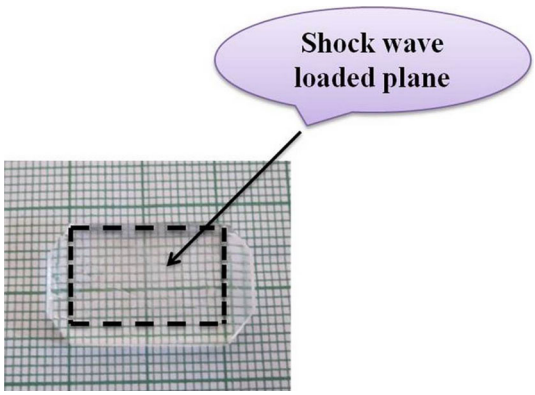

Fig. 1. Photograph of as-grown KDP single crystal.

RESULT AND DISCUSSION

Powder XRD Analysis

Powder x-ray diffraction (PXRD) is a superior method of analysis for distinguishing between the crystalline phase purity and physical phases of a crystalline material. The PXRD pattern of our KDP crystal was recorded by utilizing Rigaku mini Flux II, and predominant peaks were found at the planes (101), (200), (211), (112), (220), (202) (301), (103), (321), (312), (420), (204) and (105). The obtained Powder XRD spectrum clearly reveals that the grown KDP crystal has good crystallinity and closely matches the literature values.[28,29] The diffraction pattern of KDP crystal sample is shown in Fig. 4.

Surface Morphology Analysis

Optical microscopy was utilized to analyze the surface morphology of the KDP crystal for pre- and post-shock wave loaded conditions. Figure 5a shows the pre-shock wave loaded sample surface with water etching for 5 s. The etch pattern shows that the crystalline nature is quite good. Figure 5b shows the post-shock wave loaded KDP crystal surface, which confirms that there is no visible damage on the surface of the crystal.

Polarizing optical microscopy was employed to examine the surface morphology for both pre- and post-shock wave loaded samples, as shown in Fig. 6a and b. These images further prove that there was no damage on the surface of the shock wave loaded sample.

Dielectric Constant and Dielectric Loss

Dielectric constant and dielectric loss are basic electrical properties of materials which determine the dissociation of atoms, ions and their polarization mechanism, depending on the frequency and temperature.[30] Permittivity and permeability can be varied with frequency, temperature, orientation of atomic sites, pressure, and molecular structure of the material.[7–11] The real and imaginary parts of the electrical parameters provide crucial information about the material properties which determine the applicability of the material. The dielectric constant of a material is generally due to ionic,

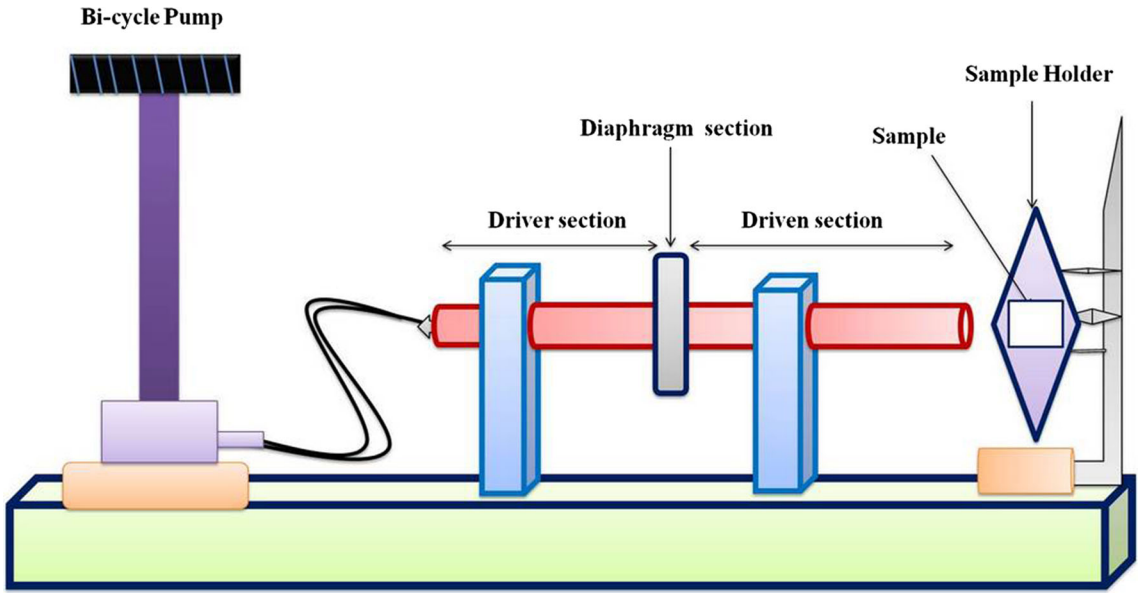

Fig. 2. Schematic diagram of experimental setup of shock wave loading on KDP crystal.

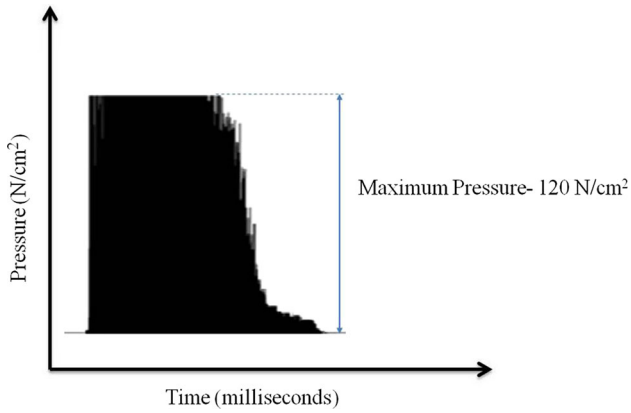

Fig. 3. Pressure profile of shock wave of Mach number 1.9.

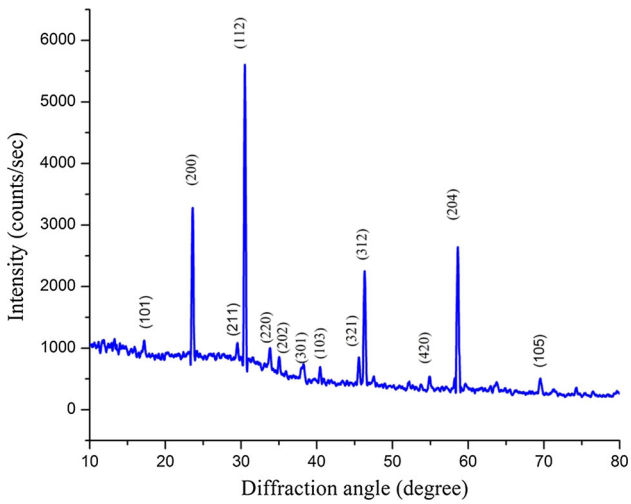

Fig. 4. Powder XRD pattern of grown KDP crystal.

electronic, orientation and space charge polarizations. In most materials, all four polarizations are active in the low frequency region and act nonlinearly in the high frequency region. The dielectric constant of a crystal is derived from the standard relation.

$$\varepsilon_r = \frac{C_p d}{\varepsilon_o A} \quad (1)$$

where ε_r, C_p, ε_o, d and A are dielectric constant, capacitance, absolute permittivity of the free space (8.85×10^{-12} F m^{-1}), thickness and area of the sample, respectively.

The demand for the low dielectric constant materials is increasing for industrial applications such as microelectronic, optoelectronic and non-linear optical devices.[24,28,31] Hence, we analyzed the dielectric properties of crystals are analyzed before and after the shock wave-loaded condition using an impedance analyzer PSM 1735 LCR meter. The voltage oscillation level was fixed at ± 2 V for the dielectric measurement. A well-polished KDP crystal of dimension of $13.11 \times 11.52 \times 3.37$ mm^3 was placed between the electrodes coated with silver paste. The resistance, capacitance, and dissipation factor were measured from the LCR meter and the dielectric constant and dielectric loss of the crystal was calculated for both pre- and post-shock wave loaded conditions. Figure 7a and b show the variation of dielectric constant and dielectric loss of the KDP crystal with respect to frequency for pre-shock wave loaded conditions and post-shock wave loaded conditions. Both the dielectric constant and dielectric loss decrease with increases of frequency. The shock wave loaded KDP crystal shows a lower dielectric constant than the normal KDP crystal because high

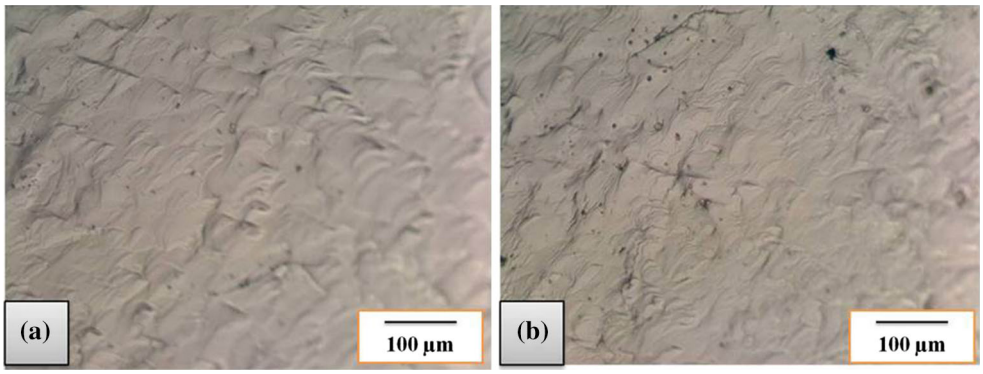

Fig. 5. Optical microscopic images of KDP crystal surfaces: (a) pre-shock wave loaded condition and (b) post-shock wave loaded condition.

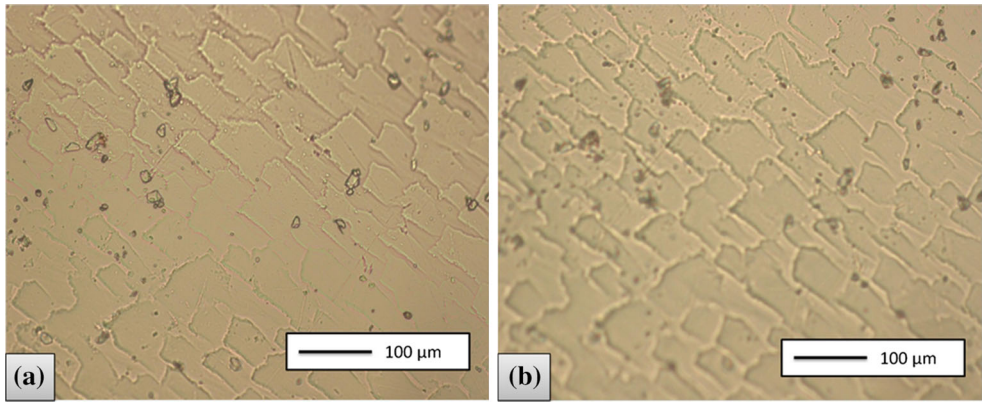

Fig. 6. Polarizing optical microscopic images of KDP crystal surfaces: (a) pre-shock wave loaded condition and (b) post-shock wave loaded condition.

pressure and high temperature from the impulse shock wave layer interact with the crystal, which leads to an increase in the restoring force and decrease in the lattice polarization, causing a reduction in the value of the dielectric constant.[32]

To better understanding these experimental investigations, at least qualitatively, various effects have to be considered in the crystal domains. In general, ferroelectric domain theory states that only 90° domains contribute to the polarization mechanism. This can be attributed to challenging of influence by the shock wave in the opposite direction of the contribution of re-polarization domains and the growth of 180° micro polar regions. From the literature, it is known that the polarization axis of KDP is along the long *c*-axis.[33] Figure 8 shows a schematic diagram of the pre- and post-shock loaded KDP crystal with polarizing dipoles in the presence of an external electric field. For example, let us consider the KDP crystal as a simple three-dimensional bulk crystal. In case of the pre-shock wave loaded condition, the KDP crystal has a greater number of polarizing dipoles in the presence of the electric field (shown in Fig. 8a). By contrast, in the post-shock wave loaded condition, the contribution of polarizing dipoles is significantly reduced (shown in the Fig. 8b). Under extreme stress and pressure conditions, the polarization of the molecules is altered.[32,34,35]

In shock wave loaded conditions, the non-90° domain walls may be enhanced, which decreases the polarization, resulting in a decrease of the dielectric constant. This reflects as a distortion disappearance of space charge polarization, decreasing the lattice polarization and effectively decreasing dipole strength; these are the causes for the low dielectric constant, since the number of dipoles and the dielectric constant are linear.[36]

Real and Imaginary Part Permittivity and Impedance

The real and imaginary parts of permittivity elucidate the energy loss of the KDP crystal before and after shock wave loading, as shown in Fig. 9a and b. From the measured values of impedance (Z), phase (θ) and the sample dimensions, we can calculate the real and imaginary parts of the permittivity using the following relations:

$$Z' = Z\cos\theta \tag{2}$$

$$Z'' = Z\sin\theta \tag{3}$$

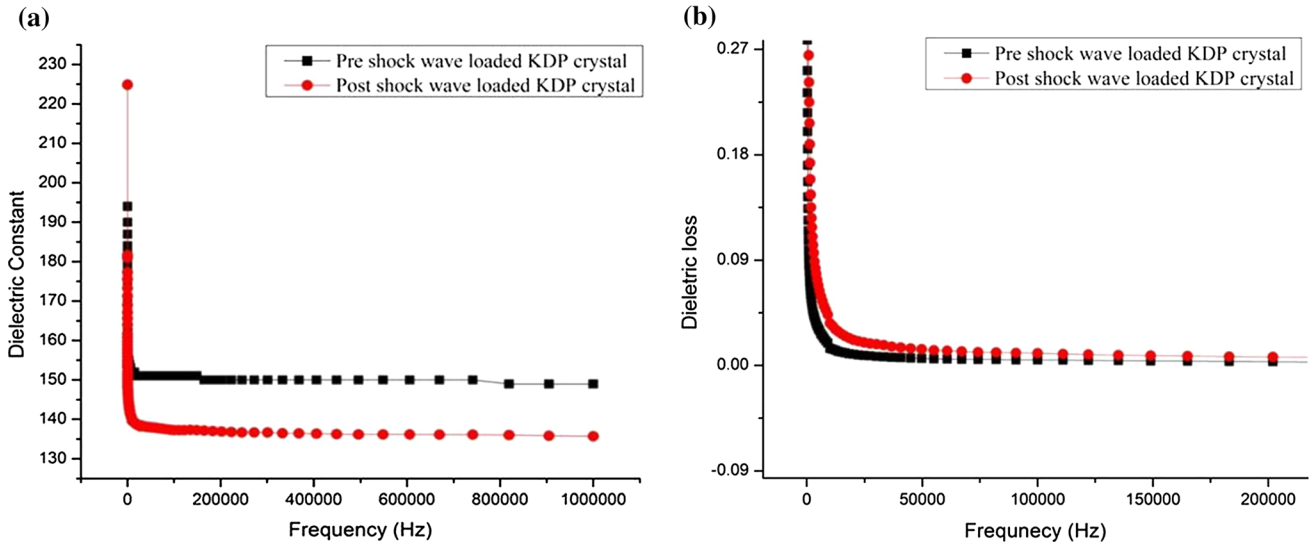

Fig. 7. (a) Dielectric constant against frequency for both pre- and post-shock wave loaded conditions of KDP crystal. (b) Dielectric loss against frequency for pre- and post-shock wave loaded conditions of KDP crystal.

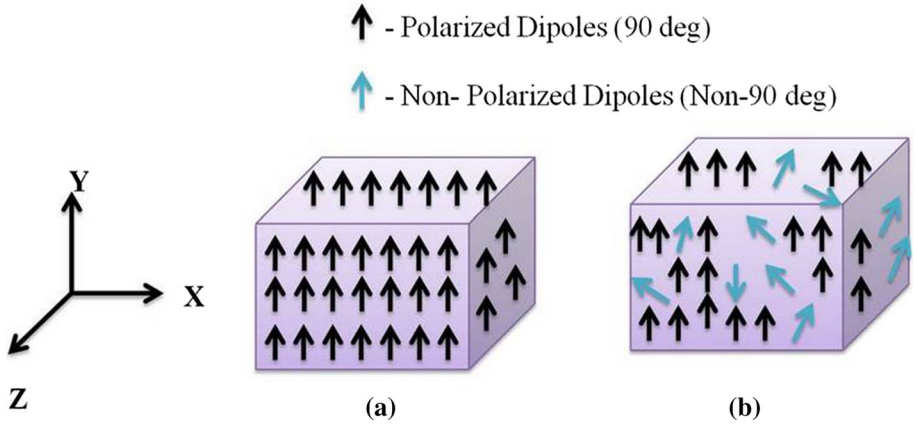

Fig. 8. Schematic diagram of the KDP crystal polarized dipoles in the external electrical field. (a) Pre-shock wave loaded KDP crystal and (b) post-shock wave loaded KDP crystal.

$$\varepsilon' = \frac{Z''}{2\pi f C_o Z^2} \tag{4}$$

$$\varepsilon'' = \frac{Z'}{2\pi f C_o Z^2} \tag{5}$$

$$C_o = \frac{\varepsilon_o A}{d} \tag{6}$$

where ε' and ε'' are the real and imaginary parts of complex relative permittivity, Z', Z'' are the real and imaginary parts of the impedance, and $C_o$and f, are the geometric capacitance and input frequency, respectively. From Fig. 9a and b, the decrease of the real part of permittivity with frequency could be attributed to the misalignment of dipole orientation along the field direction.[24] Shock wave loaded crystal shows a lower value of the real part of permittivity in comparison to pre-shock wave loaded crystal. Hence, it is clearly demonstrated that shock wave loaded KDP crystal has fewer dipoles in the presence of an electric field. On the other hand, the imaginary part of permittivity for the shock wave loaded crystal shows that there is no significant change in the shock wave loaded condition. Figures 10a and b show the difference in real and imaginary parts of impedance with frequency at room temperature. It is evident that the behavior of the real and imaginary parts of impedance are high in the lower frequency region and decrease gradually as the frequency increases; all the curves are saturated in the high frequency region for both the pre- and post-shock wave loaded crystal. This may be due to the appearance of space charge polarization in the high frequency region. The real and imaginary parts of impedance are higher for shock loaded crystal than for normal crystal.

Complex Impedance

Impedance spectrum $Z^*(\omega)$ is a complex number, comprising real and imaginary parts, which is a function of input frequency (ω), where $\omega = 2^*\pi^*f$. Complex impedance can be utilized to determine the dielectrical properties of a material.[37–39] Generally, the real part of impedance is plotted on X-axis and the imaginary part is plotted on the Y-axis of a chart to obtain a Nyquist plot or Cole–Cole plot.

$$Z*(\omega) = (Z' - iZ'') \quad (7)$$

In a Cole–Cole plot, the impedance can be represented as a vector of length $|Z|$. Phase angle is the angle between these vectors. The semicircular arc represents the characteristics of the time constant, and also indicates the parallel combination of resistance and capacitance. Normally, composite materials exhibit a non-Debye type of relaxation with continuous distribution relaxation time around the mean relaxation time.[37]

Figure 11 shows the single semicircular arc of the pre- and post-shock wave loaded crystal, demonstrating the presence of the dielectric relaxation. Radius of curvature of the Nyquist arc is directly proportional to the resistivity of the material.[30] Both pre- and post-shocked crystals exhibit a single semicircular arc, but height of the arc and radius of the semicircular arc are significantly affected by the shock loading. The post-shock loaded crystal shows a low radius of curvature and reduced curve height. The reduction in the radius of curvature of the Nyquist arc of the crystal could be due to the fast moving charge carriers. The electric conduction of the crystal is due to ionic and migrating charge carriers which move rapidly in the three-dimensional hydrogen bond network.[40] Interaction with the shock wave induces a fast response of charge carries towards the hopping phenomenon, producing good conductivity among the atomic sites which enhances the conductivity behavior of the KDP crystal. Impedance parameters from the Nyquist plots were analyzed to investigate the internal electrical resonance and the interfacial changes due to the impact of the shock pulse on the KDP crystal for pre- and post-shock loaded conditions. Figure 11 shows a semicircular arc between the frequency region of 1 Hz to 1 MHz and the exhibited semicircular arc for pre- and post-shock loaded KDP crystal, which is well fitted to the equivalent circuit [Rs $(C_1R_1)(C_2R_2)$], as shown in the inset of Fig. 11, where R_1 and R_2 are the resistances of the KDP crystal and polarization resistance or charge transfer resistance at the electrode interface, and C_1 and C_2 represents the double-layer capacitance and pseudo-capacitance, respectively, at the applied bias voltage.

The resultant resistance for pre and post shock loaded KDP crystal is found to decrease from the total resistance significantly. The semicircular arc observed for pre shock loaded KDP crystal evidenced to be apparent due to the accumulated charge transfer by the influence of bias voltage. Moreover, the trend observed for post shock loaded KDP crystal shows a decreased semicircular arc that might be due to the reflected systematic variation in R_1 and R_2 which enhances retarded dielectric relaxation generated by the recombination of charged polarons during loading of shock wave.

AC, DC Conductivity and Resistivity

AC conductivity, DC conductivity and resistivity can be characterized using the test relation

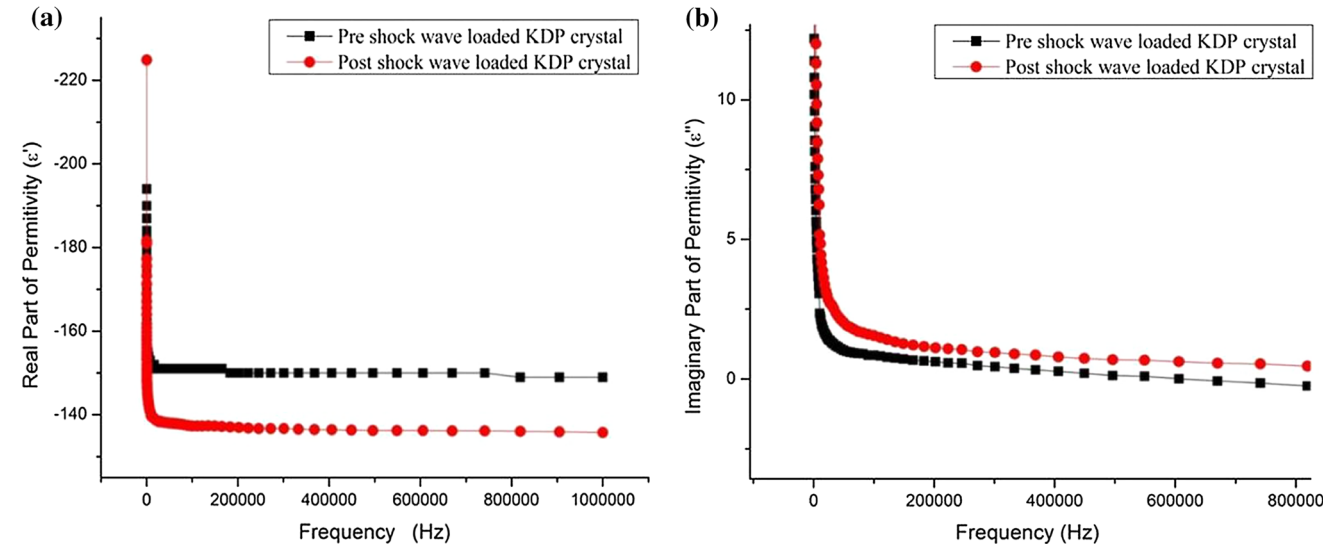

Fig. 9. (a) Plot of real part of permittivity against frequency for pre-shock wave loaded condition. (b) Plot of imaginary part of permittivity against frequency for post-shock wave loaded condition.

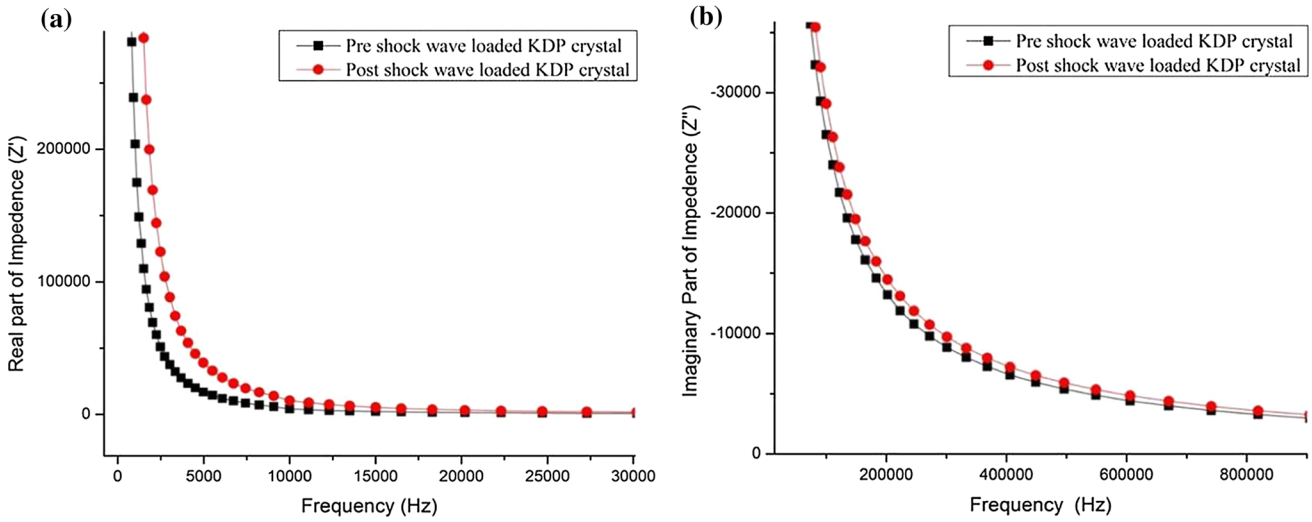

Fig. 10. (a) Plot of real part of impedance against frequency for pre-shock wave loaded condition. (b) Plot of imaginary part of impedance against frequency for post-shock wave loaded condition.

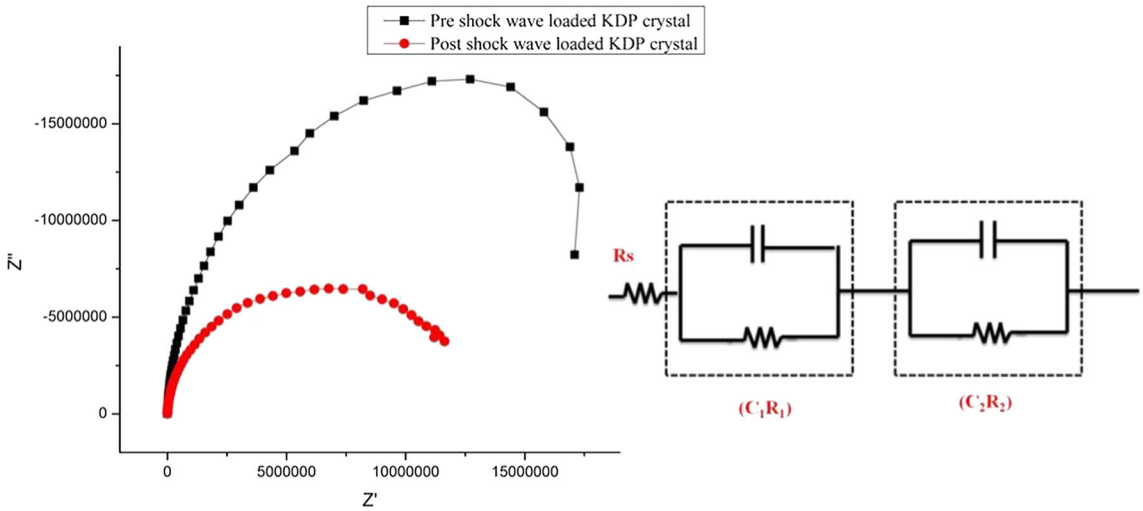

Fig. 11. Nyquist plot with impedance vector for both pre-shock wave loaded KDP crystal and post-shock wave loaded KDP crystal.

$$\sigma_{ac} = \varepsilon_r \varepsilon_o \omega \tan \delta \tag{8}$$

$$\sigma_{dc} = \frac{1}{\rho} \tag{9}$$

$$\rho = \frac{R_b}{d} \tag{10}$$

where ρ is the resistivity, ε_r is absolute permittivity in the free space (8.85×10^{-12} F m^{-1}) and $\omega = 2\pi f$ is the angular frequency, R_b is the resistance of the crystal and d is the thickness of the sample. Figures 12a, b, and c clearly show the reduction of resistivity for the shock loaded crystal, hence both AC and DC conductivity are increased. AC conductivity and DC conductivity are low for the lower frequency region and increase gradually for higher frequency and resistivity. This may be due to the fact that under high pressure and temperature, the proton tunneling modes, such as tunneling energy, hopping mechanism and mobility of the charge carriers, are enhanced.[40–42]

Capacitance

The capacitance of the crystal is measured from the following formula:

$$C_p = \varepsilon_r \varepsilon_o \frac{A}{d} \tag{11}$$

where C_p is the capacitance, in farads; A is the area, ε_r is the relative permittivity, d is thickness of the crystal and ε_o is the absolute permittivity. The capacitance value decreases, while frequency exhibits an increasing trend as shown in Fig. 13. In the

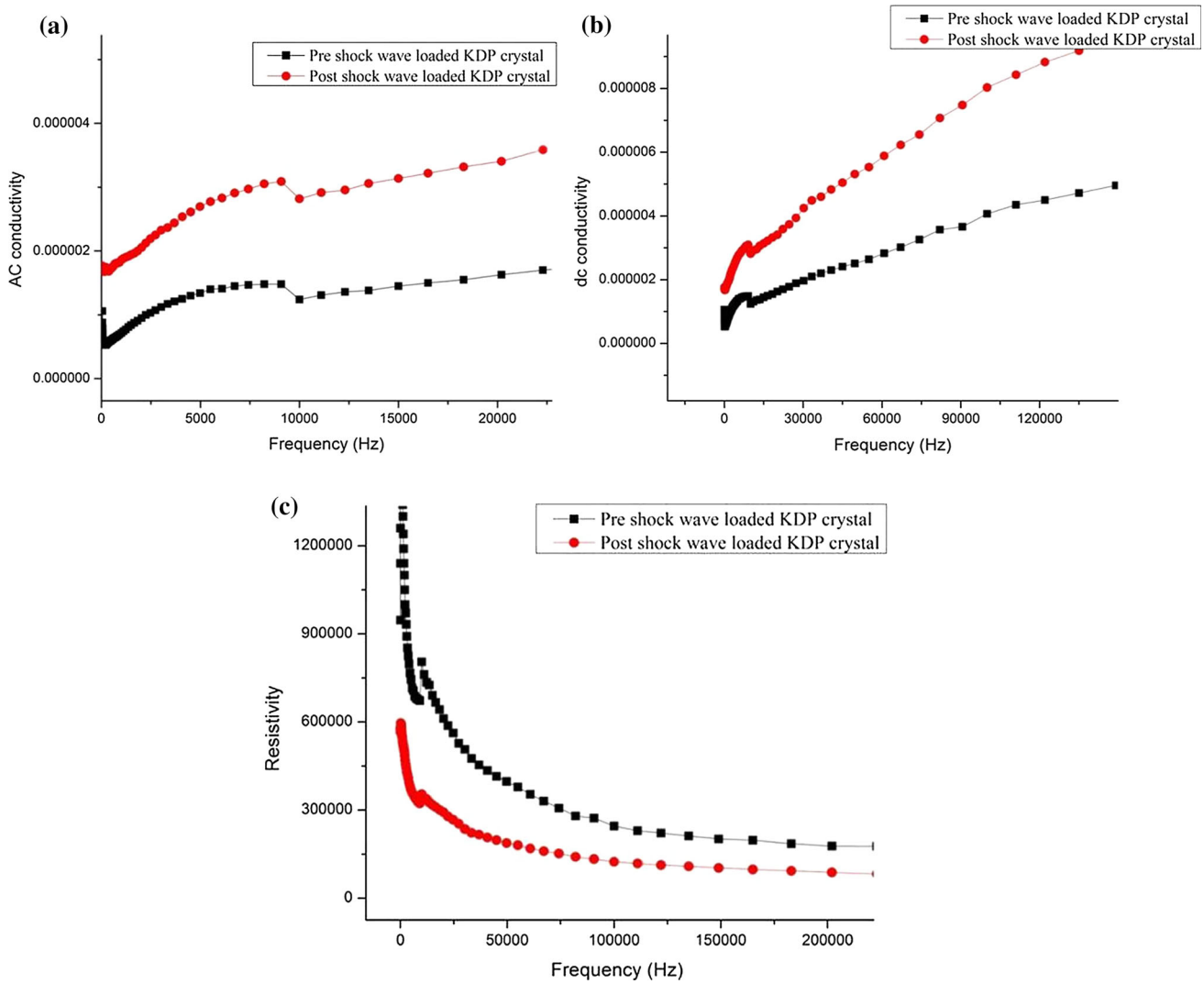

Fig. 12. (a) Plot of AC conductivity against frequency for both pre- and post-shock wave loaded crystal. (b) Plot of DC conductivity against frequency for both pre- and post-shock wave loaded crystal. (c) Plot of resistivity against frequency for both pre- and post-shock wave loaded crystal.

higher frequency region, the value of capacitance is saturated. The lower value of capacitance for shock loaded crystal indicates that shock wave impact may have reduced the number of dipoles.

Piezoelectric Studies

Piezoelectric responses of ferroelectric materials are some of the most important properties for technological applications.[43] The piezoelectric response of pre- and post-shock wave loaded KDP crystals was examined to understand the impact of shock waves on the crystal. Interestingly, both pre- and post-shock wave loaded KDP crystal showed the same piezoelectric coefficient (d_{33}) as 2 pC/N. No change was observed in the piezoelectric coefficient value for the shock wave loaded sample.

CONCLUSION

We reported an alternative approach to reducing dielectric properties of KDP crystal using a mild shock wave produced by a table-top shock tube. The proposed alternative method is safe, as it makes use of low pressure, low temperature, and is non-destructive. The results depict that the interaction of shock waves with KDP crystal alters electrical properties such as dielectric constant, dielectric loss, permittivity, impedance, AC conduction, DC conduction and capacitance. Further, the effect on the crystal for both pre- and post-shock wave loaded conditions were discussed for the said electrical parameters as a function of a spectrum of frequencies ranging from 1 Hz to 1 MHz. The experimental results reveal that the dielectric constant of KDP crystal decreases from 158 to 147, likely due to the

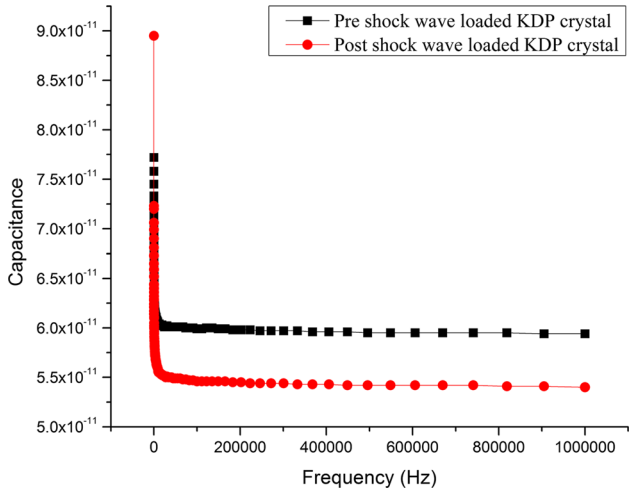

Fig. 13. Plot of capacitance against frequency for both pre- and post-shock wave loaded KDP crystal.

enhancement of non-polarized dipoles in the crystal lattice. Investigations of piezoelectric response of test materials reveal that the shock pulses do not alter the piezoelectric coefficient. Shock loaded crystal is a very suitable candidate for microelectronic and optoelectronic applications due to its low dielectric constant. The study of impact of shock waves on crystals as a function of different Mach numbers is in progress.

REFERENCES

1. R.M. Hazen and L.W. Finger, *Rev. Sci. Instrum.* 52, 75 (1981).
2. E.V. Boldyreva, N. Ivashevskaya, H. Sowa, H. Ahsbahs, and H.-P. Weber, *Z. Kristallogr.* 220, 50 (2005).
3. E.V. Boldyreva, S.N. Ivashevskaya, H. Sowa, H. Ahsbahs, and H.P. Weber, *Dokl. Phys. Chem.* 396, 111 (2004).
4. V.S. Shusta, I.P. Prits, P.P. Guranich, E.I. Gerzanich, and A.G. Silvika, *Condens. Mater. Phys.* 10, 91 (2007).
5. J. Suchanicz and K. Wojcik, *Mater. Sci. Eng. B* 104, 31 (2003).
6. V.M. Kedyulich, A.G. Silvika, E.I. Gerzanich, A.M. Guivan, and P.M. Lukach, *Condens. Mater. Phys.* 6, 271 (2003).
7. I.V. Stasyuk, R.R. Levitskii, and A.P. Monia, *Condens. Mater. Phys.* 2, 731 (1999).
8. A.A. Charakhchyana, V.V. Milyavskiib, and K.V. Khishchenko, *High Temp.* 47, 235 (2009).
9. G.I. Kanel, V.E. Fortov, and S.V. Razorenov, *Phys. Uspekhi.* 50, 771 (2007).
10. J. Zhang and P.S. Branicio, *Procedia Eng.* 75, 150 (2014).
11. V.A. Gnatyuk, T. Aoki, and Y. Hatanaka, *Appl. Phys. Lett.* 88, 242111 (2006).
12. S.-N. Luo, T.C. Germann, D.L. Tonks, and Q. An, *J. Appl. Phys.* 108, 093526 (2010).
13. D.E. Hooks, K.J. Ramos, and A. Richard, *J. Appl. Phys.* 100, 024908 (2006).
14. F. Mullar and E. Schulte, *Z. Naturforsch.* 33, 918 (1978).
15. Z.A. Derger, Y.A. Gruzdkov, Y.M. Gupta, and J.J. Dick, *J. Phys. Chem. B* 106, 247 (2002).
16. P.A. Urtiew, *J. Appl. Phys.* 45, 3490 (1974).
17. S.T. Weir, A.C. Mitchell, and W.J. Nellis, *J. Appl. Phys.* 80, 1522 (1996).
18. K. Kadau, T.C. Germann, P. Lomdahl, and B.L. Holian, *Science* 296, 1681 (2002).
19. K. Kadau, T.C. Germann, P.S. Lomdahl, R.C. Albers, J.S. Wark, A. Higginbotham, and B.L. Holian, *Phys. Rev. Lett.* 98, 135701 (2007).
20. B.P. Chandra, S. Parganiha, V.D. Sonwane, V.K. Chandra, P. Jha, and R.N. Baghe, *J. Lumin.* 178, 196 (2016).
21. S. Goma, C.M. Padma, and C.K. Mahadevan, *Mater. Lett.* 60, 3701 (2006).
22. S. Balamurugan and P. Ramasamy, *Spectrochim. Acta Part A* 71, 1979 (2009).
23. N. Pattanaboonmee, P. Ramasamy, and P. Manyum, *Procedia Eng.* 32, 1019 (2012).
24. S. Chandran, R. Paulraj, and P. Ramasamy, *Mater. Res. Bull.* 68, 210 (2015).
25. A. Majumder and Z.K. Nagy, *Chem. Eng. Sci.* 101, 593 (2013).
26. L. Zhang, Y. Wu, Y. Liu, and H. Li, *RSC Adv.* 7, 26170 (2017).
27. K.P.J. Reddy and N. Sharath, *Curr. Sci.* 104, 172 (2013).
28. K. Boopathi and P. Ramasamy, *Opt. Mater.* 37, 629 (2014).
29. M. Shkir, B. Riscob, M.A. Khan, S. AlFaify, E. Dieguez, and G. Bhagavannarayana, *Spectrochim. Acta A* 124, 571 (2014).
30. M. Manivannan, S.A. Martin Britto Dhas, and M. Jose, *J. Cryst. Growth* 455, 161 (2016).
31. P. Rajesh, A. Silambarasan, and P. Ramasamy, *Mater. Res. Bull.* 49, 640 (2014).
32. S. Mayburg, *Phys. Rev.* 79, 375 (1950).
33. H. Yurtseven and S. Sen, *Adv. Condens. Mater. Phys.* 2012, 1 (2012).
34. R. Yimnirun, S. Ananta, E. Meechoowas, and S. Wonsaennmai, *J. Phys. D Appl. Phys.* 36, 1615 (2003).
35. R. Yimnirun, S. Wongsaenmai, A. Ngamjarurojana, and S. Ananta, *Curr. Appl. Phys.* 6, 520 (2006).
36. D. Shamiryan, T. Abell, F. Iacopi, and K. Maex, *Mater. Today* 7, 34 (2004).
37. R.H. Chen, C.-C. Yen, C.S. Shern, and T. Fukami, *Solid State Ion.* 177, 2857 (2006).
38. M. Pandey, G.M. Joshi, K. Deshumkh, and J. Ahamd, *Adv. Mater. Lett.* 6, 165 (2015).
39. M.H. Khan and S. Pal, *Adv. Mater. Lett* 5, 384 (2014).
40. A. Goddat, J. Peyronneau, and J.P. Poirier, *Phys. Chem. Miner.* 27, 81 (1999).
41. Z.M. Elimat, *J. Compos. Mater.* 49, 1 (2013).
42. E. Matsushita, *Solid State Ion.* 145, 445 (2001).
43. S. Goel, N. Sinha, H. Yadav, A.J. Joseph, A. Hussain, and B. Kumar, *Arab. J. Chem.* (2017). https://doi.org/10.1016/j.arabjc.2017.03.003.